Biogerontology (2009) 10:203–211
DOI 10.1007/s10522-008-9172-4

RESEARCH ARTICLE

Dicarbonyl-induced accelerated aging in vitro in human skin fibroblasts

Henrik Sejersen · Suresh I. S. Rattan

Received: 6 August 2008 / Accepted: 14 August 2008 / Published online: 29 August 2008

Abstract Dicarbonyls glyoxal (GO) and methylglyoxal (MGO) produced during the autoxidation of reducing sugars are a source of macromolecular damage in cells. Since an accumulation of damaged macromolecules is a universal characteristic of aging, we have tested whether GO and MGO which cause oxidative damage to proteins and other macromolecules can bring about accelerated aging in normal human skin fibroblasts in vitro. A treatment of cells with 1.0 mM GO or 400 μM MGO leads to the appearance of senescent phenotype within 3 days, as judged by the following criteria: morphological phenotype, irreversible growth arrest and G_2 arrest, increased senescence-associated β-galactosidase (SABG) activity, increased H_2O_2 level, increased N^{ξ}-(carboxymethyl)-lysine (CML) protein level, and altered activities of superoxide dismutase and catalase antioxidant enzymes. This experimental model of accelerated cellular aging in vitro can be useful for studies on testing the effects of various physical, chemical and biological conditions, including natural and synthetic molecules, for the modulation of aging.

Keywords Oxidative stress · α-oxoaldehydes · Cell cycle · CML-modified proteins · Antioxidant enzymes

H. Sejersen · S. I. S. Rattan (✉)
Laboratory of Cellular Ageing, Department of Molecular Biology, University of Aarhus, Gustav Wieds Vej 10-C, 8000 Aarhus, Denmark
e-mail: rattan@mb.au.dk

Present Address:
H. Sejersen
Department of Animal Health, Welfare and Nutrition, Faculty of Agricultural Sciences, University of Aarhus, 8830 Tejle, Denmark
e-mail: Henrik.Sejersen@agrsci.dk

Introduction

An imbalance in the intracellular glucose metabolism leads to increased levels of its oxidative breakdown products such as the dicarbonyls glyoxal (GO), methylglyoxal (MGO), 3-deoxyglucosone (3-DG) and glucosone, which belong to the chemical group of α-oxoaldehydes. The main source of GO and MGO formation is the autoxidation of reducing sugars and lipid peroxidation (Wolff and Dean 1987). The dicarbonyls attack the amino groups of proteins, nucleotides and lipids with their highly reactive carbonyl groups. They are capable of reacting with lysine, arginine and cysteine residues to form irreversible advanced glycation endproducts (AGE) associated with the browning and fluorescence of proteins (Ahmed et al. 1997). Many intracellular proteins accumulate glycation adducts during aging, and some AGEs are thought to be recognition factors

for specific receptor molecules and contribute to the post-translational modification of proteins (Brownlee et al. 1984). Many age-related pathologies such as Alzheimer's disease and diabetes are associated with the accumulation of altered proteins (Rattan 2008a).

GO and MGO treatment correlates with increased intracellular reactive oxygen species (ROS) levels (Ahmed et al. 1997). The release of metal ions as a result of oxidative stress results in the homolytic cleavage of H_2O_2 to HO^- (hydroxyl radicals) and hydroxyl ion via the so-called Fenton reaction. It is not known how metal ions are released during oxidative stress, but co-incubation of glucose and bovine ceruloplasmin results in a time-dependent release of Cu^{2+} (Islam et al. 1995). It has been shown that 1 or 5 mM GO treatment in rat hepatocytes increased the ROS levels in a dose and time dependent manner (Shangari and O'Brien 2004). In addition, experimentally increased levels of H_2O_2 have been shown to increase the intracellular levels of GO and MGO in murine P388D1 macrophages, likely as a consequence of decreased in situ activity of glyoxalase-1 (Abordo et al. 1999). The exact cytotoxic mechanism of GO and MGO induced ROS production is not known but it has been proposed that toxicity might involve GO or formaldehyde adduct formation at complex I and III in the mitochondria electron transport chain (ETC), promoting the release of superoxide anion (Shangari et al. 2003).

In a pilot study published previously we had reported the dose response curves for the effects of GO on the survival and growth of normal human skin fibroblasts (Sejersen and Rattan 2007). Furthermore, it was observed that a treatment of early passage young fibroblasts with 1.0 mM GO for 3 days changed their morphology similar to that of late passage senescent cells. Therefore, we have further investigated the effects of GO and MGO treatment on human skin fibroblasts with respect to their abilities to induce accelerated aging and premature senescence, the results of which are presented here. The following criteria of aging in treated cells are studied: morphological phenotype, irreversible cell cycle arrest, reduced level of apoptosis, increased senescence-associated β-galactosidase (SABG) activity, increased H_2O_2 level, increased N^{ξ}-(carboxymethyl)-lysine (CML) protein level, and altered activities of superoxide dismutase and catalase antioxidant enzymes.

Materials and methods

Chemicals and antibodies

The following chemicals were purchased: 2′,7′ Dichlorodihydro-fluorescein diacetate (DCDHF diacetate) from Molecular Probes; 5-Dodecanoylaminofluorescein di-D-galactopyranoside (C_{12}FDG) from Imagene Green; RNase A from Roche Diagnostics; Sulfanilic acid from Acros Organics. If not specified otherwise, all other chemicals were purchased from Sigma-Aldrich. The following antibodies, purchased commercially, have been applied: anti-β-actin from Sigma-Aldrich (A5441); monoclonal anti-CML from BioLogo (CML011, clone CMS-10); anti-mouse immunoglobulins, HRP conjugated from DAKO (P0260); polyclonal anti-mouse immunoglobulins, FITC conjugated from DAKO (F0261).

Cell culture and treatment with GO and MGO

Cultures of normal human adult skin fibroblasts, designated ASF-2, were established from the breast biopsy specimen of a consenting young healthy Danish woman, and were serially passaged at 1:2 or 1:4 split ratio, as described previously (Rattan and Sodagam 2005; Sejersen and Rattan 2007). At about 90% confluency the cell culture was split using the trypsin/EDTA method (BioWhittacker™, Cambex Bio Science). All experiments were performed with ASF-2 cells at population doubling levels between 7 and 53, which represent 15–100% replicative lifespan completed in vitro. Unless otherwise stated, 100,000 cells were seeded per well in a six-well plate (growth area 9.6 cm^2) and allowed to grow for 24 h before any treatment was given.

SABG activity–histochemical staining and flow cytometric analysis

Histochemical staining

The cells were fixed at 25°C for 5 min with 2% formaldehyde in 0.2% glutaraldehyde and subsequently washed 2× with PBS. The cells were left in staining solution (Dimri et al. 1995) at 37°C without CO_2 for 24 h. At least 400 cells were counted three times in different areas of the well.

Flow cytometric analysis

Sample preparations were performed as described (Kurz et al. 2000). The activity of β-galactosidase was measured by adding 33 μM of the fluorogenic substrate C_{12}FDG followed by incubation for 1 h. The cells were washed with ice-cold PBS at the end of incubation, resuspended by trypsinization and analyzed immediately using a flow cytometer. The living cells were gated using FSC/SSC and changes reported as mean fluorescence intensities (MFI). ASF-2 cells of 100% completed lifespan were included in the assay as a positive control. The FACSCalibur cytometer from Becton Dickinson (BD) Biosciences was applied for analysis. Cell Quest Pro (BD) was used for data acquisition and FlowJo from TreeStar for data analysis and final layout.

Cell cycle analysis

The cells were trypsinized 72 h after GO or MGO treatment. Approximately 1×10^6 cells/sample were spun down at 300*g* for 5 min, fixed at 4°C for 1 h with fridge-cold 70% ethanol, and 100 μl of RNase A (100 μg/ml DNase free) added before incubation at 37°C without CO_2 for 15 min. The suspension was subsequently left at 25°C for 1 h after the addition of 400 μl PI (50 μg/ml in PBS). The samples were analyzed with a flow cytometer. The living cells were gated using FSC/SSC and cell aggregates were gated out via so-called pulse processing, using PI-height/PI-area. The G_1/G_0, S and G_2/M phases were defined with the Watson Pragmatic model fit (Watson et al. 1987).

H_2O_2 detection by flow cytometry

The cells were trypsinized 4 h after treatment with GO or MGO. Approximately 1×10^6 cells were incubated with 2 μM DCDHF diacetate at 25°C in the dark for 1 h. DCF fluorescence was determined by analyzing 0.5×10^6 cells with a flow cytometer (excitation wavelength, 488 nm; emission wavelength, 515–545 nm). The living cells were gated using FSC/SSC and changes reported as mean fluorescence intensities (MFI).

CML-protein detection by flow cytometry

The cells were trypsinized 72 h after GO or MGO treatment and fixed with 0.25% paraformaldehyde at 4°C for 20 min followed by another fixation step in fridge cold 70% methanol at 4°C for 1 h. The cells were permeabilized on ice in 0.25% Triton® X-100 for 5 min. Approximately 1×10^6 cells were stained by adding 100 μl of anti-CML antibody from Biologo (25 ng/ml). The cells were incubated with primary antibody at 25°C for 30 min and reincubated with 100 μl of FITC-conjugated anti-mouse solution (diluted 1:5) in the dark at 25°C for 30 min. The cells were analyzed immediately after last incubation with a flow cytometer. The living cells were gated using FSC/SSC and changes reported as mean fluorescence intensities (MFI). Auto-fluorescence and isotype controls were tested with a positive control of CML-modified cells. The anti-CML antibody was tested for specificity using BSA-CML and BSA-CEL standards followed by conventional western blotting. No BSA-CEL binding was detected, as expected (Koito et al. 2004). The CML modified cells, BSA-CML and BSA-CEL were made by incubation in a proper reaction mixture, as described previously (Reddy et al. 1995; Ahmed et al. 1997).

SOD activity assay

SOD activity was measured with a kit (SOD Assay Kit, BioVision). The lysate buffer contained 0.05 M Tris/HCl [pH 8], 0.15 M NaCl, 0.01 M $MgCl_2 \cdot 6H_2O$, 10% glycerol, 0.0025% SDS and protease inhibitors (Protease Inhibitor Cocktail, Sigma-Aldrich). Each test sample contained the necessary blanks according to the kit protocol. The samples were incubated with WST solution at 37°C for 20 min before the absorbance was read at 450 nm using a microplate reader. The SOD activity (inhibition rate %) was calculated and the protein content determined by a conventional Lowry protein assay. All samples were normalized to total protein content and the activities at 4 h further normalized to the activities at 0 h.

Catalase activity assay

The catalase activity was measured with a kit (Amplex® Red Catalase Assay Kit, Molecular Probes). The fluorescence values were inverted in order to set the intercept of the standard curve to zero (1/fluorescence). Each test sample contained a control without H_2O_2 and a second control without the

Amplex Red Reagent. The samples were incubated with 40 μM H_2O_2 on a shaker at 25°C for 30 min. About 200 μl Amplex Red Reagent was added before starting the fluorescence measurement on a PolarStar Optima fluorometer from BMG Labtech (excitation wavelength, 544 nm; emission wavelength, 590 nm; 15 cycles; 120 s/cycle; 30 min). The protein content was determined by a conventional Lowry protein assay and all samples were normalized to total protein content. The activities at 4 h were further normalized to the activities at 0 h.

Results

Cell morphology and SABG activity

Early-passage ASF-2 cells (with less than 50% lifespan completed) were treated with 1.0 mM GO or 400 μM MGO, and were observed during a period of 24–72 h for changes in morphology and cell growth. The selection of doses was made on the basis of our pilot study published previously (Sejersen and Rattan 2007). Figure 1 (panel A) shows that as compared with the controls, the cells treated with either GO or MGO for 72 h became enlarged, irregularly shaped, flattened, and vacuolated, giving the appearance of typically senescent cells as described in biogerontological literature (Cristofalo et al. 2004; Rattan 2008b; Xie et al. 2008). These carbonyl-induced changes in cell morphology from young to senescent were irreversible, since the removal of GO and MGO from the culture medium did not result in any significant reversion in appearance to young morphology during the next 72 h of maintenance (Fig. 1, panel B).

GO- and MGO-treated cells were further analyzed for the appearance of senescent cells by SABG activity assay, by both histochemical staining and flow cytometery. A 72 h of treatment increased the proportion of β-galactosidase positive cells from 5.5% in the controls to 43% and 11.6% in GO- and MGO-treated cultures, respectively, as determined by conventional staining protocol (Dimri et al. 1995) and by counting at least 400 cells in each set up (pictures not shown). In order to confirm the semi-quantitative analysis, another analysis for SABG activity using flow cytometery was performed. Figure 2 shows that a 72 h treatment of early passage ASF-2 cells with GO or MGO increased their SABG activity relative to control samples.

Cell cycle analysis

Effects of GO and MGO on the cell cycle parameters of ASF-2 cells were determined by flow cytometery. Figure 3a shows that whereas the untreated control cultures had 5.5 ± 0.5% of the cells in the G_2/M phase of the cell cycle, the GO- or MGO-treated cultures had significantly increased proportions (27.5 ± 0.7% and 38.2 ± 1.5%, respectively) of the cells arrested in G_2/M phase. Furthermore, GO- and MGO-treated cultures showed a shift in the forward scatter to the right (Fig. 3b), which is indicative of

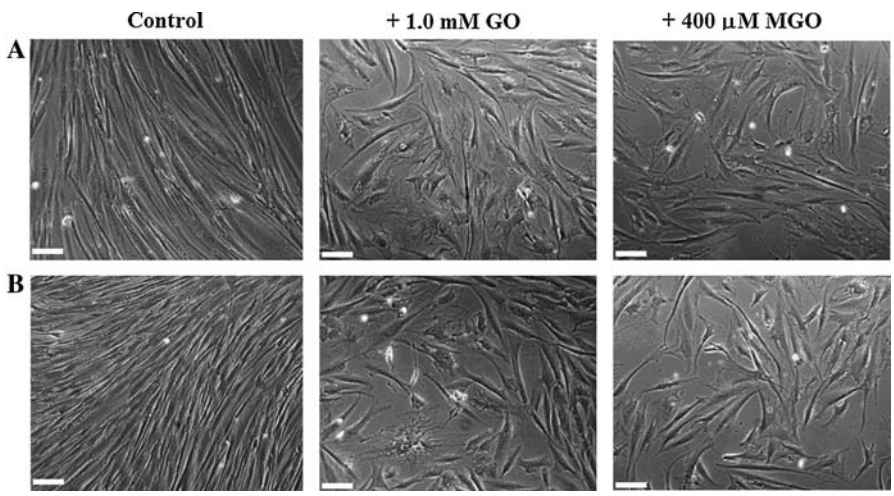

Fig. 1 Effect of GO and MGO on the morphology of early passage young human skin fibroblasts. (**a**) Induction of senescent phenotype within 72 h of treatment with 1 mM GO or 400 μM MGO. (**b**) Lack of reversibility of GO- and MGO-induced premature senescent phenotype after the removal of GO and MGO for 72 h. Bar: 100 μm

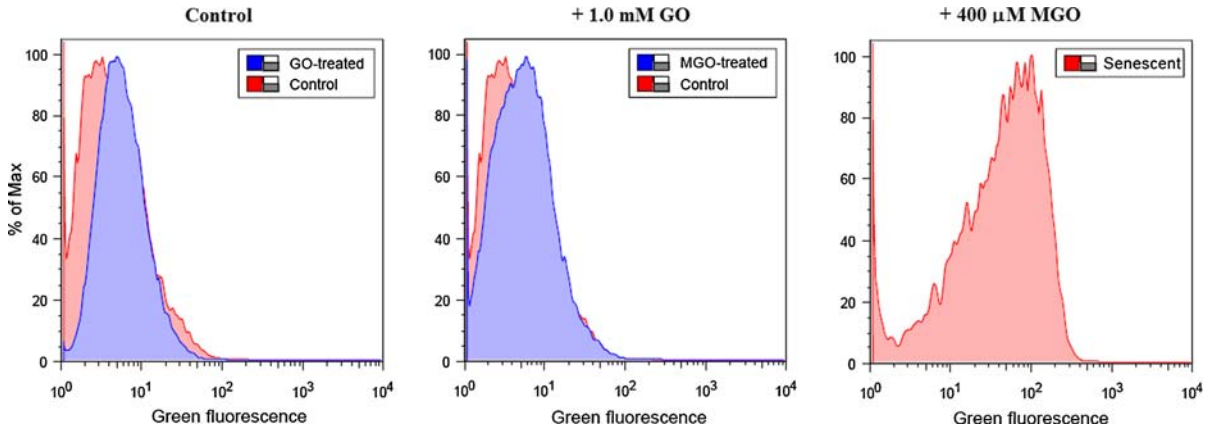

Fig. 2 SABG activity of GO- or MGO-treated human skin fibroblasts, measured by flow cytometry and C_{12}FDG fluorescence, which emits green light when cleaved by β-galactosidase. The auto-fluorescence of each sample was less than the output shown but slightly higher for the GO-treated and scenescent cultures

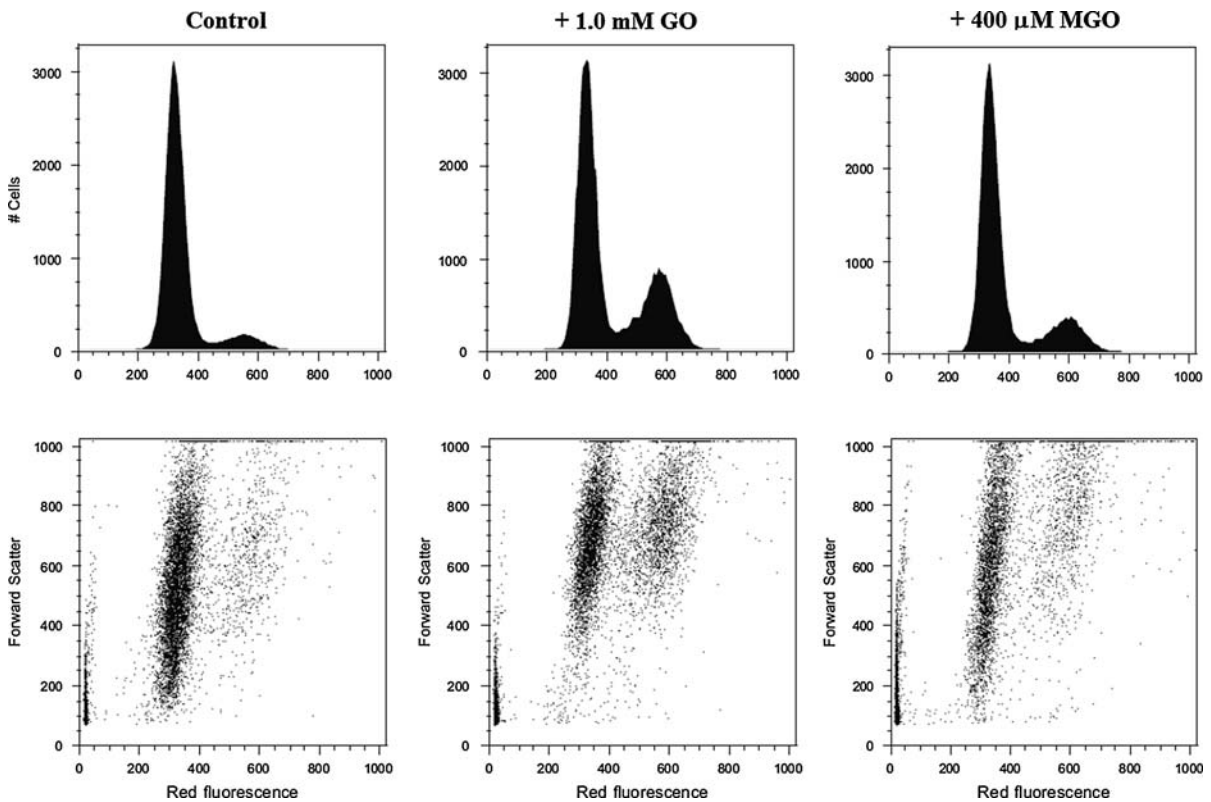

Fig. 3 Cell cycle analysis of GO- or MGO-treated human skin fibroblasts. (**a**) Relative DNA content, as measured by PI staining. (**b**) Dot plot of PI against FSC shift ($n = 3$, $P < 0.05$ between control and treated cells)

increased cell size. This increase in the proportion of cells arrested in G_2/M phase, and an increase in cell size was not accompanied by an increase in the extent of apoptotic cell death, as measured by AnnexinV/PI-staining in flow cytometery (data not shown).

Induction of oxidative damage and antioxidative enzymes

Flow cytometric estimation of intracellular levels of H_2O_2, as measured by DCF formation, in GO- and

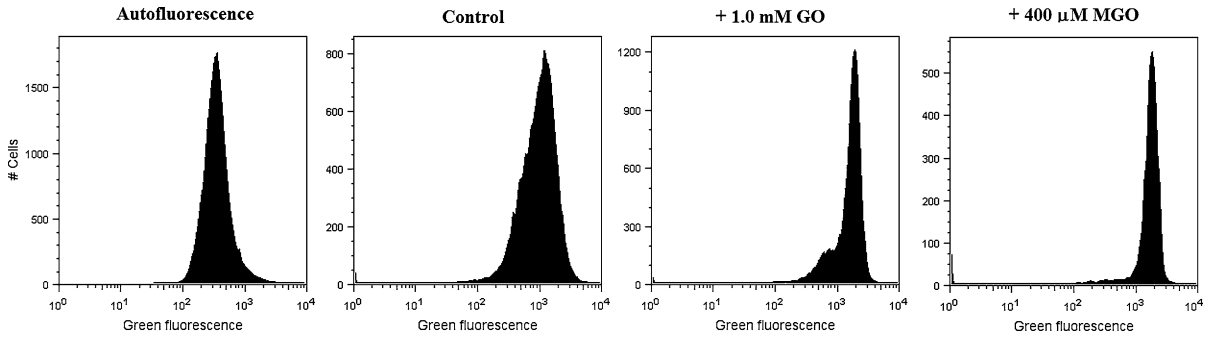

Fig. 4 Levels of H_2O_2 4 h after GO or MGO treatment in early-passage human skin fibroblasts. A representative of the autofluorescence is shown

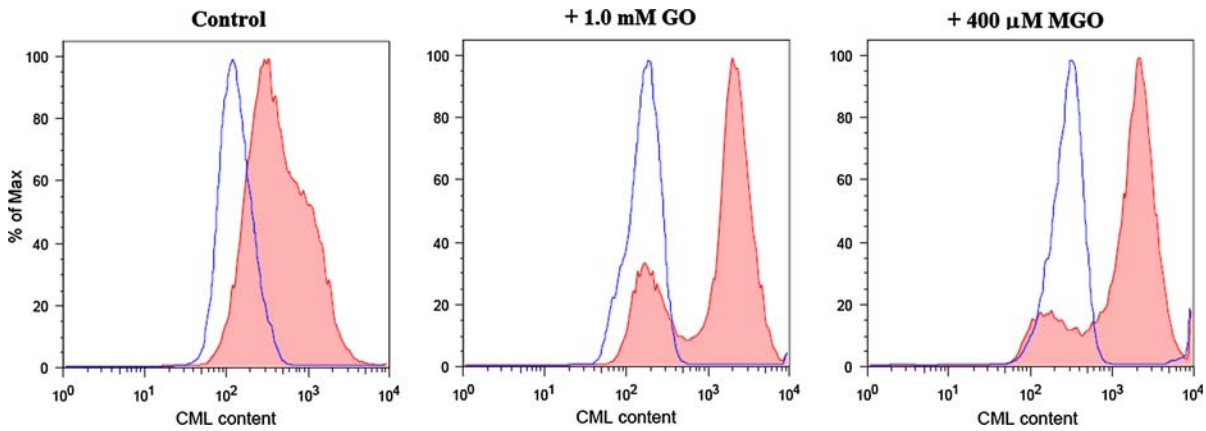

Fig. 5 Total CML-protein level 72 h after GO or MGO treatment of early-passage human skin fibroblasts (blue, unstained; red, stained)

MGO-treated cells showed a 2-fold of increase after 4 h of treatment (Fig. 4). The presence of CML-modified proteins after 72 h of GO or MGO treatment was approximately 5-fold higher than that in untreated cells, respectively (Fig. 5).

The enzyme activities of SOD and catalase were determined at the time of treatment (0 h) and 4 h after GO or MGO treatment in early-passage cells. Figure 6 shows that both SOD and catalase activities were significantly enhanced, but only in MGO-treated cells relative to the control cells. No further increase in either ROS level or catalase and SOD activities were detected 72 h after dicarbonyl treatment. The increased enzyme activities in MGO-treated cells match the increased ROS level within the same period.

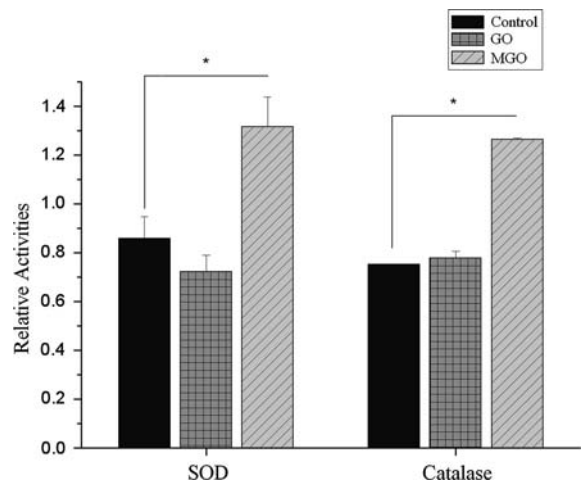

Fig. 6 Relative SOD and catalase activities in early passage human skin fibroblasts after GO or MGO treatment for 4 h ($n = 3$, $^*P < 0.05$)

Discussion

We have demonstrated that a treatment of early-passage human skin fibroblasts with 1.0 mM GO or 400 μM MGO results in accelerated aging and the appearance of the senescent phenotype. The outcome of GO- and MGO-treatment is similar to other characteristics of serially passaged replicative senescence, such as cell morphology, irreversible growth arrest, increased SABG activity, increased H_2O_2 level, and an increased level of oxidatively damaged CML-proteins.

Senescence and irreversible proliferate arrest of cells can be caused by various stresses, including oxidative damage (Collado and Serrano 2006). However, serially passaged cells are known to get G_1-arrested at the onset of replicative senescence and enter a viable G_0/G_1-end state (Tsutsui et al. 2002). G_1 and G_2 arrest can also be induced by ionizing radiation and treatment with various mutagens. For example, cells can become G_2/M arrested in a methylator-induced, mismatch repair-dependent manner (Adamson et al. 2005). In the context of H_2O_2 treatment it has been demonstrated that cells in the S phase commit to apoptosis, whereas the G_1 and G_2/M cells commit to growth arrest (Chen and Goligorsky 2006).

GO and MGO are strong electrophiles capable of damaging the DNA. GO- and MGO-induced DNA damage is one factor likely to contribute to the G_2 arrest, but we have not observed any significant level of DNA strand breaks within the first 12 h of GO- or MGO-treatment, as measured by the comet assay (data not shown). However, GO and MGO may induce other oxidative DNA damage such as 8-hydroxy-2′-deoxyguanosine (8-OHdG) (Kasai et al. 1998). Another form of specific DNA damage is the accelerated telomere shortening in response to stress (Epel et al. 2004). The stress-induced senescence by H_2O_2 is typically independent of telomere shortening and cannot be prevented by ectopic hTERT (human telomerase reverse transcriptase) expression in fibroblasts (Ben-Porath and Weinberg 2004; Gorbunova et al. 2002). Therefore, it is most likely that dicarbonyl-induced premature senescence is also telomere-independent. This, however, needs to be verified experimentally.

The main cause of GO- or MGO-induced G_2-arrest may be the cytoskeletal protein damage, inhibiting cytokinesis. Cells are normally arrested in the G_0/G_1 phase as they become senescent. This difference between the G_0/G_1 and G_2/M arrest can be explained by the large amount of protein damage occurring in cells treated with very high concentrations of GO or MGO relative to normal endogenous steady-state levels of the same molecules. The G_2 arrest can be applied as a marker of cellular damage and a good marker of GO- and MGO-induced skeletal protein damage.

The two-fold increase in H_2O_2 levels 4 h after treatment is a sign of ongoing oxidative stress in GO- or MGO-treated cells, although the exact mechanisms of GO- and MGO-induced H_2O_2 formation are unclear. GO and MGO might inhibit the electron transport chain in the mitochondria by direct modification of complex I and III, leading to electron leakage. The subsequent inhibition of mitochondrial respiration at complex IV, where O_2 is reduced to H_2O, is responsible for an increase in the O_2 pool, which in turn increases the formation of O_2^- at complex I and III (Shangari and O'Brien 2004). An increased level of ROS is correlated to GSH depletion, increasing the level of lipid peroxidation, glucose autoxidation, AGE and ALE formation. In addition, GO has been shown to inhibit glutathione reductase (GR) (Shangari et al. 2006), reducing the level of GSH and in turn GO and MGO detoxification by the cytosolic glyoxalase system.

CML-modified proteins as well as other AGEs are good molecular markers of aging because they accumulate during normal aging *in vivo* (Hipkiss 2006; Kueper et al. 2007). In our studies the observation that there is a significant increase in CML-proteins is additional evidence supporting the induction of accelerated aging in GO- and MGO-treated human fibroblasts.

As regards antioxidant systems against oxidative stress, several enzymes, including superoxide dismutase (SOD), catalase, glutathione peroxidase, and G6PDH are capable of scavenging reactive oxygen species (Niwa et al. 1993). Over expressing CuZn-SOD in V79 Chinese hamster cells reduced the H_2O_2 steady-state levels, supporting the hypothesis that O_2^- dismutation prevents the formation of higher H_2O_2 levels by other reactions (Teixeira et al. 1998). CuZn-SOD is located in the peroxisomes where it converts $2O_2^-$ into H_2O_2 and O_2 using Cu and Zn as cofactors (Keller et al. 1991). In our studies SOD and catalase activities were significantly enhanced in MGO-treated cells relative to the control cells. This was

expected since the level of H_2O_2 increased 4 h after treatment. The activity enhancement could reflect an upregulation of the SOD and catalase genes or a posttranslational activation by unknown mechanisms. The SOD and catalase activities, however, were unchanged in GO-treated cells. GO has been shown to inhibit glutathione reductase (GR), an enzyme involved in the reduction of glutathione (GSSG to GSH) (Shangari and O'Brien 2004). GO might inhibit GR indirectly by NADPH depletion (Shangari et al. 2003). The lower activity of SOD in GO-treated samples is most likely linked to a specific cytotoxic mechanism of GO. Alternatively, the rate of SOD and possibly catalase inhibition might be different in GO- or MGO-treated cells. Both GO and MGO treatments have been shown to reduce the intracellular level of GSH (Abordo et al. 1999). The higher activities of SOD and catalase in MGO-treated cells, however, are indicative of ongoing oxidative stress.

Finally, we have established a novel model system of the so-called stress-induced premature senescence (SIPS) (Toussaint et al. 2002), using dicarbonyl metabolites of glucose. Such a model system can be useful for testing various conditions which may modulate the process of aging positively or negatively. In addition, the well known relationship between altered glucose metabolism and various pathologies, including those involving the accumulation of damaged and abnormal proteins, further strengthens the usefulness of dicarbonyl-induced accelerated aging system as an experimental system. Our studies are in progress exploring various possibilities of using this system for testing the effects of natural and synthetic molecules and other conditions in the induction and prevention of cellular aging in cancerous and normal cells, respectively.

Acknowledgments We thank Dr. Peter Kristensen for his interest and useful suggestions made during the course of these studies. Thanks to Helle Jakobsen and Gunhild Siboska for their technical assistance; to Alexander Schmitz for help in the FACS analysis; and to Cristovao Lima for performing the comet assay. The Laboratory of Cellular Ageing is supported by research grants from the Danish Medical Research Council (FSS), and EU's Biomed Health Programme, Proteomage.

References

Abordo EA, Minhas HS, Thornalley PJ (1999) Accumulation of alpha-oxoaldehydes during oxidative stress: a role in cytotoxicity. Biochem Pharmacol 58:641–648. doi:10.1016/S0006-2952(99)00132-X

Adamson AW, Beardsley DI, Kim WJ, Gao Y, Baskaran R, Brown KD (2005) Methylator-induced, mismatch repair-dependent G2 arrest is activated through Chk1 and Chk2. Mol Biol Cell 16:1513–1526. doi:10.1091/mbc.E04-02-0089

Ahmed MU, Brinkmann Frye E, Degenhardt TP, Thorpe SR, Baynes JW (1997) N-epsilon-(carboxyethyl)lysine, a product of the chemical modification of proteins by methylglyoxal, increases with age in human lens proteins. Biochem J 324(Pt 2):565–570

Ben-Porath I, Weinberg RA (2004) When cells get stressed: an integrative view of cellular senescence. J Clin Invest 113:8–13

Brownlee M, Vlassara H, Cerami A (1984) Nonenzymatic glycosylation and the pathogenesis of diabetic complications. Ann Intern Med 101:527–537

Chen J, Goligorsky MS (2006) Premature senescence of endothelial cells: Methusaleh's dilemma. Am J Physiol Heart Circ Physiol 290:1729–1739. doi:10.1152/ajpheart.01103.2005

Collado M, Serrano M (2006) The power and the promise of oncogene-induced senescence markers. Nat Rev Cancer 6:472–476. doi:10.1038/nrc1884

Cristofalo VJ, Lorenzini A, Allen RG, Torres C, Tresini M (2004) Replicative senescence: a critical review. Mech Ageing Dev 125:827–848. doi:10.1016/j.mad.2004.07.010

Dimri GP, Lee X, Basile G, Acosta M, Scott G, Roskelley C et al (1995) A biomarker that identifies senescent human cells in culture and in aging skin in vivo. Proc Natl Acad Sci USA 92:9363–9367. doi:10.1073/pnas.92.20.9363

Epel ES, Blackburn EH, Lin J, Dhabhar FS, Adler NE, Morrow JD et al (2004) Accelerated telomere shortening in response to life stress. Proc Natl Acad Sci USA 101:17312–17315. doi:10.1073/pnas.0407162101

Gorbunova V, Seluanov A, Pereira-Smith OM (2002) Expression of human telomerase (hTERT) does not prevent stress-induced senescence in normal human fibroblasts but protects the cells from stress-induced apoptosis and necrosis. J Biol Chem 277:38540–38549. doi:10.1074/jbc.M202671200

Hipkiss AR (2006) Accumulation of altered proteins and ageing: causes and effects. Exp Gerontol 41:464–473. doi:10.1016/j.exger.2006.03.004

Islam KN, Takahashi M, Higashiyama S, Myint T, Uozumi N (1995) Fragmentation of ceruloplasmin following non-enzymatic glycation reaction. J Biochem 118:1054–1060

Kasai H, Iwamoto-Tanaka N, Fukada S (1998) DNA modifications by the mutagen glyoxal: adduction to G and C, deamination of C and GC and GA cross-linking. Carcinogenesis 19:1459–1465. doi:10.1093/carcin/19.8.1459

Keller GA, Warner TG, Steimer KS, Hallewell RA (1991) Cu, Zn superoxide dismutase is a peroxisomal enzyme in human fibroblasts and hepatoma cells. Proc Natl Acad Sci USA 88:7381–7385. doi:10.1073/pnas.88.16.7381

Koito W, Araki T, Horiuchi S, Nagai R (2004) Conventional antibody against Nepsilon-(carboxymethyl)lysine (CML) shows cross-reaction to Nepsilon-(carboxyethyl)lysine (CEL): immunochemical quantification of CML with a

specific antibody. J Biochem 136:831–837. doi:10.1093/jb/mvh193

Kueper T, Grune T, Prahl S, Lenz H, Welge V, Biernoth T et al (2007) Vimentin is the specific target in skin glycation structural prerequisites, functional consequences, and role in skin aging. J Biol Chem 282:23427–23436. doi:10.1074/jbc.M701586200

Kurz DJ, Decary S, Hong Y, Erusalimsky JD (2000) Senescence-associated (beta)-galactosidase reflects an increase in lysosomal mass during replicative ageing of human endothelial cells. J Cell Sci 113(Pt 20):3613–3622

Niwa Y, Iizawa O, Ishimoto K, Akamatsu H, Kanoh T (1993) Age-dependent basal level and induction capacity of copper-zinc and manganese superoxide dismutase and other scavenging enzyme activities in leukocytes from young and elderly adults. Am J Pathol 143:312–320

Rattan SI (2008a) Increased molecular damage and heterogeneity as the basis of aging. Biol Chem 389:267–272

Rattan SI (2008b) Cell senescence in vitro. In: Encyclopedia of the Life Sciences. Wiley: Chichester. doi: 10.1002/9780470015902.a0002567.pub2

Rattan SI, Sodagam L (2005) Gerontomodulatory and youth-preserving effects of zeatin on human skin fibroblasts undergoing aging in vitro. Rejuvenation Res 8:46–57. doi:10.1089/rej.2005.8.46

Reddy S, Bichler J, Wells-Knecht KJ, Thorpe SR, Baynes JW (1995) N epsilon-(carboxymethyl)lysine is a dominant advanced glycation end product (AGE) antigen in tissue proteins. Biochemistry 34:10872–10878. doi:10.1021/bi00034a021

Sejersen H, Rattan SI (2007) Glyoxal-induced premature senescence in human fibroblasts. Ann NY Acad Sci 1100:518–523. doi:10.1196/annals.1395.057

Shangari N, O'Brien PJ (2004) The cytotoxic mechanism of glyoxal involves oxidative stress. Biochem Pharmacol 68:1433–1442. doi:10.1016/j.bcp.2004.06.013

Shangari N, Bruce WR, Poon R, O'Brien PJ (2003) Toxicity of glyoxals-role of oxidative stress, metabolic detoxification and thiamine deficiency. Biochem Soc Trans 31:1390–1393

Shangari N, Chan TS, Popovic M, O'Brien PJ (2006) Glyoxal markedly compromises hepatocyte resistance to hydrogen peroxide. Biochem Pharmacol 71:1610–1618. doi:10.1016/j.bcp.2006.02.016

Teixeira HD, Schumacher RI, Meneghini R (1998) Lower intracellular hydrogen peroxide levels in cells overexpressing CuZn-superoxide dismutase. Proc Natl Acad Sci USA 95:7872–7875. doi:10.1073/pnas.95.14.7872

Toussaint O, Remacle J, Dierick JF, Pascal T, Frippiat C, Royer V et al (2002) Stress-induced premature senescence: from biomarkers to likeliness of in vivo occurrence. Biogerontology 3:13–17. doi:10.1023/A:1015226524335

Tsutsui T, Kumakura S, Yamamoto A, Kanai H, Tamura Y, Kato T et al (2002) Association of p16(INK4a) and pRb inactivation with immortalization of human cells. Carcinogenesis 23:2111–2117. doi:10.1093/carcin/23.12.2111

Watson JV, Chambers SH, Smith PJ (1987) A pragmatic approach to the analysis of DNA histograms with a definable G1 peak. Cytometry 8:1–8. doi:10.1002/cyto.990080101

Wolff SP, Dean RT (1987) Glucose autoxidation and protein modification. The potential role of 'autoxidative glycosylation' in diabetes. Biochem J 245:243–250

Xie L, Pandey R, Xu B, Tsaprailis G, Chen QM (2008) Genomic and proteomic profiling of oxidative stress response in human diploid fibroblasts. Biogerontology. doi:10.1007/s10522-008-9157-3